

Light transport behaviours in quasi-1D disordered waveguides composed of random photonic lattices

Yuchen Xu, Hao Zhang*, Yujun Lin and Heyuan Zhu

Shanghai Ultra-precision Optical Manufacturing Engineering Center,

Department of Optical Science and Engineering,

Fudan University, Shanghai 200433, China

*zhangh@fudan.edu.cn

Abstract

We present a numerical study on the light transport properties which are modulated by the disorder strength in quasi-one-dimensional disordered waveguide which consists of periodically arranged scatterers with random dielectric constant. The transport mean free path is found to stay inversely proportional to the square of the relative fluctuation of the dielectric constant as in the 1D and 2D cases but with . The transport properties of light through a sample with a fixed size can be modulated from ballistic to localized regime as well, and a generalized scaling function is defined to determine the light transport status in such a sample. The calculation of the diffusion coefficient and the energy density profile of the most transmitted eigenchannel clearly exhibits the transition of transport behaviour from diffusion to localization.

1 Introduction

Transport in random media at the mesoscopic scale has attracted much attention in recent decades. In the multiple scattering process, wave interference persists and leads to a series of extraordinary phenomena in contrast to common diffusion, such as Anderson localization and enhanced backscattering[1, 2, 3]. Anderson localization predicts exponentially localized modes and a halt of diffusion when the disorder reaches a certain extent, while enhanced backscattering manifests itself as the precursor of Anderson localization showing an intensity enhancement factor of 2 in the opposite direction of the incident wave due to constructive interference[4]. About two decades after Anderson localization was predicted, a single-parameter

scaling theory of localization was proposed[5]. It defines a universal scaling function $\beta(g) = d \ln g / d \ln L$ which shows how the electronic dimensionless conductance g of a random system decreases with the incremental system length L , without directly considering the disorder strength of the system.

Experimental observations of Anderson localization have been realized so far for matter waves[6, 7, 8], elastic media[9] and photons[4, 10, 11, 12, 13, 14]. Among these, the experiments carried out by Schwartz et. al. adopted a real-time induction method to form two-dimensional photonic lattices with controlled disorder in a dielectric crystal, and showed the variation of the transport from ballistic to diffusive by increasing the disorder strength, and transverse localization is definitely observed when the disorder is strong enough[13]. This reminds us that, one can take advantage of the disorder-modulation other than changing the length scale of the sample to investigate the transport properties in random media.

For a fixed sample size L in quasi-one-dimension (quasi-1D), the light propagation through a random media mainly depends on some length scales, especially the transport mean free path (TMFP) l_{tr} . l_{tr} is the critical length scale over which the incident wave loses its initial direction. It is also the fundamental parameter measuring the disorder of a random medium which only depends on the disorder strength and the incident wavelength. The relation of l_{tr} , L and the localization length ξ determines which transport regime does the system belong to. Therefore, the study on the transport mean free path should be in the first place when investigating the transport properties of random media.

Investigation of transmission, based on the transmission matrix t of the system, however, enables us to acquire comprehensive understanding on the transport properties of random media. The optical counterpart of the electronic dimensionless conductance g , i.e., the transmittance T , can be expressed as the sum of all the transmission eigenvalues as $T = \sum_{n=1}^N \tau_n$, where $\{\tau_n\}$ are the transmission eigenvalues lying within the range from 0 to 1 (full transmission) and N is the number of transverse modes. τ_n can be obtained from the singular value decomposition of the transmission matrix $t = \sum_{n=1}^N \mathbf{u}_n \sqrt{\tau_n} \mathbf{v}_n^\dagger$, with \mathbf{u}_n and \mathbf{v}_n the transmission eigenchannels composing the incoming and outgoing modes[15]. In the ballistic regime, T satisfies the macroscopic transport theory, while in the diffusive regime, $T \propto N l_{tr} / L$, and when T is close to unity, the system is about to fall into localized regime, where the eigenchannel with the maximal transmission eigenvalue dominates. The transmittance T thus gives an overall description of the transport properties.

Since the sample length is finite, the diffusion within the sample reveals position-dependent characteristics[16, 17]. For a finite sample, the variation of disorder may influence the local diffusion coefficient $D(x)$ since the diffusion related parameter l_{tr} is modulated.

In this paper, we first investigate the relation between the TMFP l_{tr} and the variant disorder strength with the sample length L fixed in a quasi-1D disordered waveguide using the exact Anderson disorder model. With l_{tr} determined, the wave transport properties including the transmittance $\langle T \rangle$ and the diffusion coefficient $D(x)$ are calculated to show the transport regime transition with the increasing disorder and verify the feasibility of modulating the transport behaviour in a periodical lattice of scatterers with random dielectric constant.

2 Numerical Methods

Consider a quasi-one-dimensional (quasi-1D) disordered sample (locally 2D) of length L and width w , with two identical semi-infinite free waveguides attached to its both ends, which are non-reflective due to the dielectric constant matching, and the transverse boundaries of the entire system is perfectly reflective, as shown in Fig. 1. A monochromatic light wave $E(x, y) \exp(-i\omega t)$ of z -polarization propagating along the x -direction is governed by the Helmholtz equation

$$\nabla^2 E(x, y) + k^2[1 + \mu(x, y)]E(x, y) = 0, \quad (1)$$

where $k = \sqrt{\varepsilon}k_0$ is the wave vector, with ε the dielectric constant of the free waveguide, $k_0 = \omega/c$ the wave vector in vacuum, respectively, and $\mu(x, y) = \delta\varepsilon(x, y)/\varepsilon$ is the relative fluctuation of the dielectric constant, which induces the disorder of the sample.

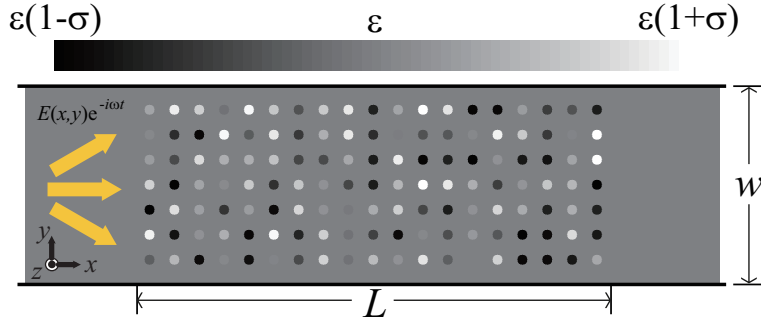


Figure 1: Schematic of the Quasi-1D waveguide considered in the simulations.

The quantized eigenstates of an empty waveguide are

$$\varphi_n^{(\pm)}(x, y) = \frac{1}{\sqrt{k_n}} \chi_n(y) e^{\pm i k_n x}, \quad (2)$$

where k_n is the longitudinal wave vector, $\chi_n(y)$ is the transverse wave function, the positive integer $n(1 \leq n \leq N)$ is the index of the eigenchannel, where $N \propto kw$

is the total number of the eigenchannels. The factor $k_n^{-1/2}$ here ensures that each channel carries normalized flux. Under the perfect reflection boundary condition, the transverse wave function takes the form

$$\chi_n(y) = \sqrt{\frac{2}{w}} \sin\left(\frac{n\pi y}{w}\right) \quad (3)$$

and the corresponding longitudinal wave vector is

$$k_n = \sqrt{k^2 - \left(\frac{n\pi}{w}\right)^2}. \quad (4)$$

The transmission matrix t can be calculated with the relation[18]

$$t_{ba}(x, x') = \sqrt{v_b v_a} \int_0^w dy \int_0^w dy' \chi_b^*(y) G^r(x, y; x', y') \chi_a(y'). \quad (5)$$

Here $t_{ba}(x, x')$ is the element of $t(x, x')$ (transmission matrix from one surface at x' to another surface at x) which represents the complex field transmission amplitude from the incoming channel a to the outgoing channel b . G^r is the retarded Green's function. v_n is the group velocity at the incident wavelength of the n^{th} channel.

In the Anderson disorder model[1], the waveguide is discretized into a square lattice with the coordinate discretization $x \rightarrow n_x d, y \rightarrow n_y d$, where d is the lattice constant. The disordered region corresponds to $1 \leq n_x \leq N_x, 1 \leq n_y \leq N_y$, where $N_x = L/d, N_y = w/d$. In the simulations $k_0 d$ is set to unity. In this basis, Eq. (5) can be written in a compact form as

$$t^{n_x, n'_x} = \frac{1}{d} V^\dagger X^\dagger G^{n_x, n'_x} X V, \quad (6)$$

where $V = \text{diag}\{v_n^{1/2}\}$ is the diagonal matrix whose diagonal elements are the group velocities of the eigenchannels and $X = [\chi_{n_y n}]_{N_y \times N}$ is the matrix whose columns are the discretized transverse wave functions of the eigenchannels. G^{n_x, n'_x} is the entire Green's function connecting the slices indexed by n_x and n'_x , which can be calculated using the recursive Green's function (RGF) method[19, 20]. Since advanced Green's function is not used here, the superscript "r" denoting retarded Green's function is omitted without ambiguity. To calculate the total transmission matrix through the whole disordered region, one just need to take $n_x = N_x + 1$ and $n'_x = 0$ in Eq. (6).

The local diffusion coefficient $D(x)$ can be calculated with the first Fick's law

$$\langle J(x) \rangle = -D(x) \frac{d \langle W(x) \rangle}{dx}, \quad (7)$$

where $J(x)$ is the energy flow, $W(x)$ is the local energy density, and $\langle \cdots \rangle$ represents ensemble average. Since there is no absorption, the energy flow is conserved and $J(x)$ is replaced by a constant J_0 . $W(x)$ can be calculated by

$$W(x) = \sum_{n,n'} |t(x,0)\mathbf{v}_n]_{n'}|^2, \quad (8)$$

where $t(x,0)\mathbf{v}_n$ is the local field at x induced by the n^{th} incoming channel.

3 Results and Discussions

Since the transport mean free path l_{tr} depends on the disorder strength of the sample and the incident wavelength, thus l_{tr} is determined by $\mu(x, y)$ when k is fixed. By applying the Anderson disorder model, $\mu(x, y)$ is quantized to μ_i on the site i in a square lattice. $\{\mu_i\}$ are independent and identically distributed random variables, therefore they satisfy

$$\langle \mu_i \mu_j \rangle = \begin{cases} \frac{\sigma^2}{3} \delta_{ij}, & \mu_i \sim U(-\sigma, \sigma) \\ \sigma^2 \delta_{ij}, & \mu_i \sim N(0, \sigma) \end{cases} \quad (9)$$

where $U(-\sigma, \sigma)$ stands for the uniform distribution and $N(0, \sigma)$ stands for the standard normal distribution, and for both distributions, obviously, $\langle \mu_i \rangle = 0$.

In the localized regime, the ensemble average of the logarithmic transmittance is proportional to the sample length and inversely proportional to the localization length ξ , i.e., $\langle \ln T \rangle = -2L/\xi$. Based on the Anderson disorder model, and for both cases of distribution of μ_i , $\langle \ln T \rangle$ is calculated at 8 different sample lengths for each value of σ , where the average is performed over a sub-ensemble of 2000 disordered configurations. By fitting the slope of $\langle \ln T \rangle$, we obtain the localization lengths, and the transport mean free paths can be extracted from the Thouless relation $\xi = (\pi/2)Nl_{\text{tr}}$, where the channel number N equals to 5. The calculated TMFPs are shown in Fig. 2 as solid circles for the uniform distribution and empty circles for the normal distribution of μ_i .

In the limit case $\sigma = 0$, the sample is actually a perfect crystal with an infinite transport mean free path. According to the Green's function theory for quantum transport[21], the mean free path is inversely proportional to the imaginary part of the self-energy $\text{Im}\Sigma^R(k)$, where the superscript R represents the retarded Green's function. The self-energy is proportional to the correlation function $\langle \mu_i^2 \rangle$, thus the mean free path is inversely proportional to the correlation function, i.e., $l_{\text{tr}}^{-1} \propto \langle \mu_i^2 \rangle$. The mean free paths for the uniform distribution and the normal distribution are linearly fitted separately, and the fitted slopes are 0.4825 and 1.518, respectively. The two slopes shows a difference factor ≈ 3 which results from the the correlation

function of the variation in the dielectric constant for different distributions as indicated by Eq. (9). l_{tr} is inversely proportional to σ^2 as predicted by theory, i.e., $l_{\text{tr}} = l_0 \sigma^{-2}$, where l_0 is the TMFP for $\sigma = 1$, which equals to $24/(\pi \varepsilon k) \simeq 2.264/k_0$ for 2D systems and $12/(\pi \sqrt{\varepsilon} k) \simeq 1.698/k_0$ for 1D systems with μ_i uniformly distributed[22]. However, our simulation obtains $l_0 \simeq 2.073/k_0$, which is between the values for 2D and 1D cases. This implies that light loses its initial direction faster in a quasi-1D (locally 2D) disordered waveguide than in a 2D one due to the transverse confinement of the perfectly reflecting boundaries.

Since the light localization length is very large in samples with very weak disorder, it will take much time to calculate the TMFP in a long sample. The linear relation of l_{tr} and σ^{-2} for optical disordered systems obtained herein can improve the computation efficiency especially for weakly disordered system by considering a relatively short sample with strong disorder.

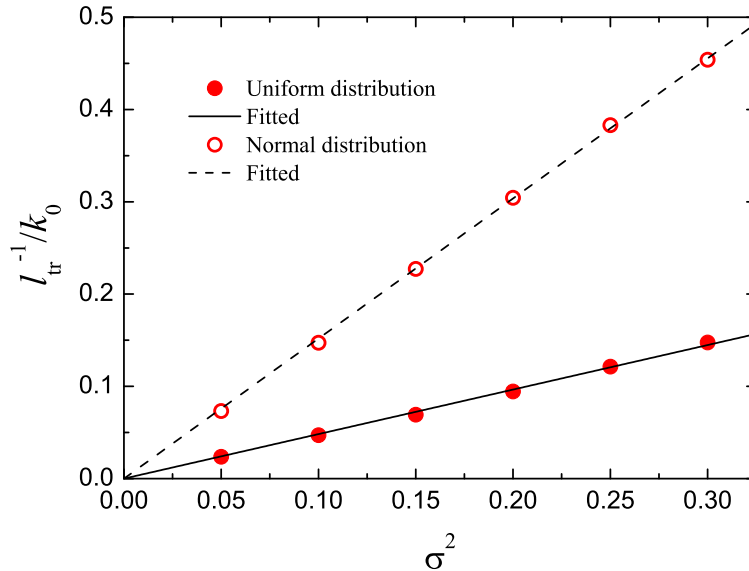


Figure 2: Transport mean free path of a disordered sample in a waveguide with $N = 5$ channels ($w = 9/k_0$) and the environment dielectric constant $\varepsilon = 2.25$, for relative dielectric constant fluctuation of a uniform distribution within $[-\sigma, \sigma]$ (solid circles) and a normal distribution with a standard deviation σ (hollow circles), which are fitted proportionally (solid line for the former and dashed line for the latter).

With the TMFP determined, the average transmittance $\langle T \rangle$ as a function of the disorder strength σ is calculated and shown in Fig. 3 for 4 different sample lengths (only consider the uniformly distributed μ_i from now on). The simulated results are compared with the consistent results of several theoretical methods

which expand $\langle T \rangle$ as [23, 24, 25]

$$\langle T \rangle \simeq g_0 - \frac{1}{3} + \frac{1}{45g_0} + \frac{2}{945g_0^2} + \mathcal{O}\left(\frac{1}{g_0^3}\right), \quad (10)$$

where

$$g_0 = \frac{N}{1 + 2L/\pi l_{\text{tr}}} \quad (11)$$

is the bare conductance. Eq. (10) is only valid in the diffusive transport regime, i.e., $l_{\text{tr}} < L \ll \xi$, and in Eq. (11) the extrapolation length z_0 induced by the internal reflection at the two end of the disordered waveguide is taken into account and its value is $\pi l_{\text{tr}}/4$. It should be emphasized that, with l_0 determined by fitting the linear relation between l_{tr}^{-1} and σ^2 before, there is no adjustable parameter in the fitting process herein. As shown in Fig. 3, the theoretical results fit well with our simulation results in the diffusive regime, which in turn verifies our results of the TMFP.

When σ is close to zero, i.e., in the ballistic and sub-diffusive regimes, the deviation of Eq. (10) from the simulation results is most obvious and mainly comes from the second term $-1/3$ (not negligible compared to the relatively small channel number N considered here), which is a signal effect of the weak-localization correlation [23] and is absent when scattering is very weak. In this case, the leading term of Eq. (10), i.e., the bare conductance g_0 is enough to describe the transmission behaviour.

For $L = 40/k_0$ (Fig. 3(a)) and $L = 100/k_0$ (Fig. 3(b)), the wave transport never really enters the localized regime ($L \gg \xi$). For $L = 200/k_0$ (Fig. 3(c)), the transport can cover the three regimes with σ tuned from 0 to 0.5, and for $L = 400/k_0$, it enters the localized regime at a smaller value of σ about 0.25. This value corresponds to a maximal fluctuation of the refractive index of about 0.2, which can be easily realized by doping randomly distributed scatterers into common optical materials and is also promising in systems of periodically arranged scatterers with random refractive index (close to our simulation model).

The classical scaling function $\beta(T)$ defined in Ref. [5] is obtained by taking the derivative $d \ln T / d \ln L$ (the angular brackets $\langle \dots \rangle$ representing the ensemble average is dropped for simplicity), but with the disorder strength fixed at $\sigma = 0.5$ and the channel number fixed at $N = 5$, which is plotted in line in Fig. 4. When L is fixed, it is straightforward to generalize the scaling function by including the variant σ as

$$\beta'(T) = \frac{d \ln T}{d \ln L'}, \quad (12)$$

where $L' = L\sigma^2$ is the effective sample length. When the transport is ballistic, T increases to N with a gradually vanishing increasing rate when σ decreases to 0,

which results that $\beta'(T)$ increases to 0 at $\ln T = \ln N$, as can be seen in Fig. 4. The vanishing point of $\beta'(T)$ moves right when N increases, which means that the scaling behaviour is influenced by the width of the sample as well.

In the localized regime, T is of the form $T = T_a \exp(-\gamma L')$, where T_a is some critical transmittance of order unity and $\gamma \propto 1/Nl_0$. Thus $\beta'(T)$ for $T \rightarrow 0$ can be derived as

$$\lim_{T \rightarrow 0} \beta'(T) = \ln(T/T_a), \quad (13)$$

as is shown in Fig. 4 for $\ln T \lesssim -2$. $\beta'(T)$ obtained from simulations for 4 different sample lengths is plotted in Fig. 4 with discrete markers. The coincidence of the line and the markers shows that it is equivalent to describe the transport status using $\beta'(T)$ and $\beta(T)$ and L' determines the transmission for a fixed N , which confirms the feasibility of the generalization of the scaling function.

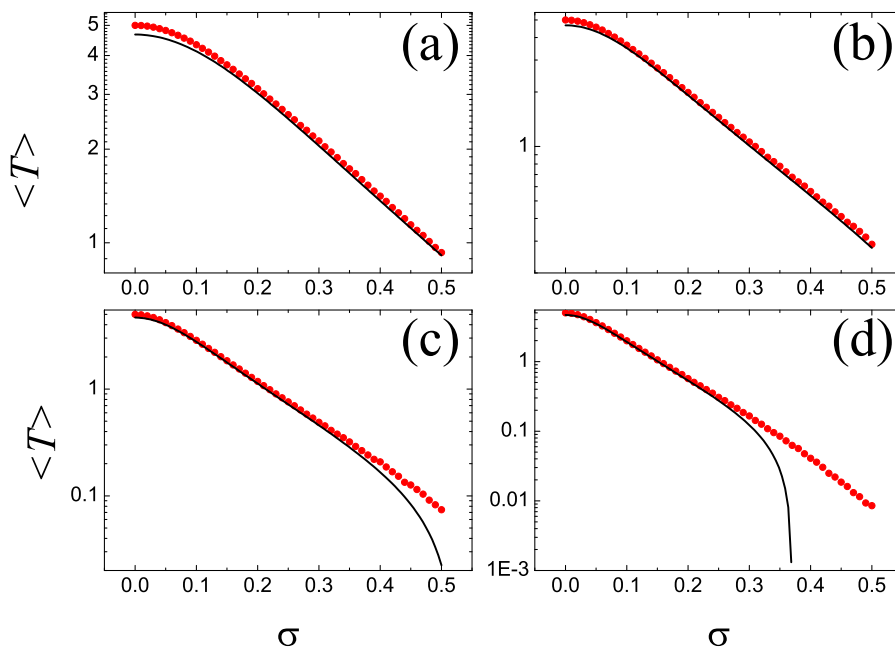


Figure 3: Dependence of transmittance $\langle T \rangle$ on the disorder strength σ within the range $[0, 0.5]$ for four different sample lengths (a) $L = 40/k_0$; (b) $L = 100/k_0$; (c) $L = 200/k_0$; (d) $L = 400/k_0$. The environmental dielectric constant is $\varepsilon = 2.25$ and the channel number is $N = 5$.

The distribution of light energy density and the local diffusion coefficient can describe the light transport behaviour through random media of different disorder strength in detail. The calculated energy density profiles $W(x)$ and the local diffusion coefficients $D(x)$ (normalized by $D(0)$) for different disorder strength are

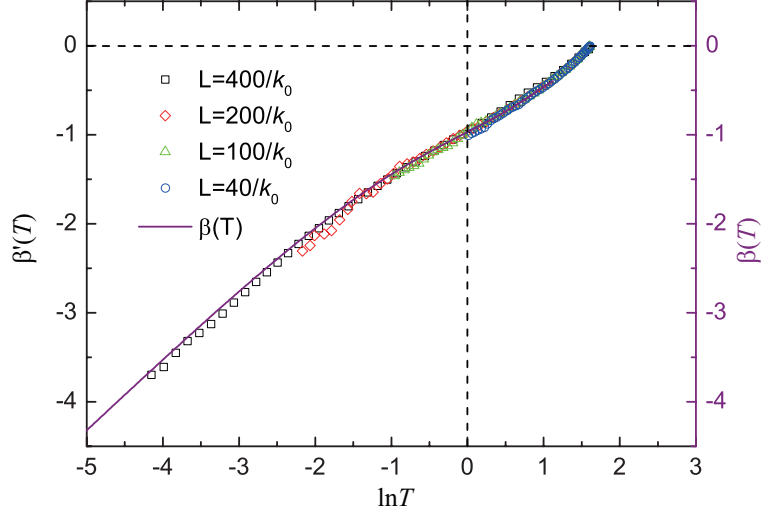


Figure 4: The generalized scaling function $\beta'(T)$ calculated for samples with channel number $N = 5$ and dielectric constant $\varepsilon = 2.25$. The blue circles, green triangles, red diamonds and black squares indicate sample length $40/k_0$, $100/k_0$, $200/k_0$ and $400/k_0$, respectively. As a comparison, the classical scaling function is plotted in line.

shown in Fig. 5(a) and (b), respectively, with the sample length fixed at $L = 400/k_0$, and 20,000 realizations taken to perform the ensemble average.

As shown in Fig. 5(a), the ensemble-averaged energy density monotonically decreases from the incident boundary to the output boundary, despite the value of σ . The backscattering of light leads to the decrease of energy density along the transport direction. Open boundaries of the sample cause energy leakage from them and the inhomogeneity of light interference. When near the boundaries, energy leaks out more easily and the interference is weaker. The descending rate keeps invariant when the disorder is very weak, e.g., for $\sigma = 0.05$, since the scattering is very weak and the energy scattered out from the boundaries is negligible. Thus the case for $\sigma = 0.05$ is a classical diffusive process with a constant diffusion coefficient, which is confirmed in Fig. 5(b). When σ increases, the interference inhomogeneity and the energy leakage is strengthened and becomes significant, which make the descending rate of the energy density become position-dependent.

Diffusion coefficients are obtained from the negative inverse derivative of the energy densities, as shown in Fig. 5(b). When the disorder is very weak, the diffusion coefficient is position-independent, while as the disorder strength increases, position-dependence emerges due to the facts that the wave interference is inhomogeneous and the returning probability becomes larger when gradually leaving the surface deepening into the sample. The position-dependence of the diffusion

coefficient is a signal of localization[16, 17].

The energy density profile $W_{\tau_1}(x)$ (for single disorder configuration) of the eigenchannel with the maximal transmission eigenvalue τ_1 also qualitatively but directly exhibits the evolution of the transport from diffusion to localization, as shown in Fig. 6. For $\sigma^2 = 0.01$ (the uppermost curve), the energy density is extended through the whole disordered region, while for $\sigma^2 = 0.25$ (the nethermost curve), the energy density is localized in a short range along the x -direction. Fig. 6 thus gives an intuitive view of the process of turning a diffusive disordered sample into a localized one by increasing σ .

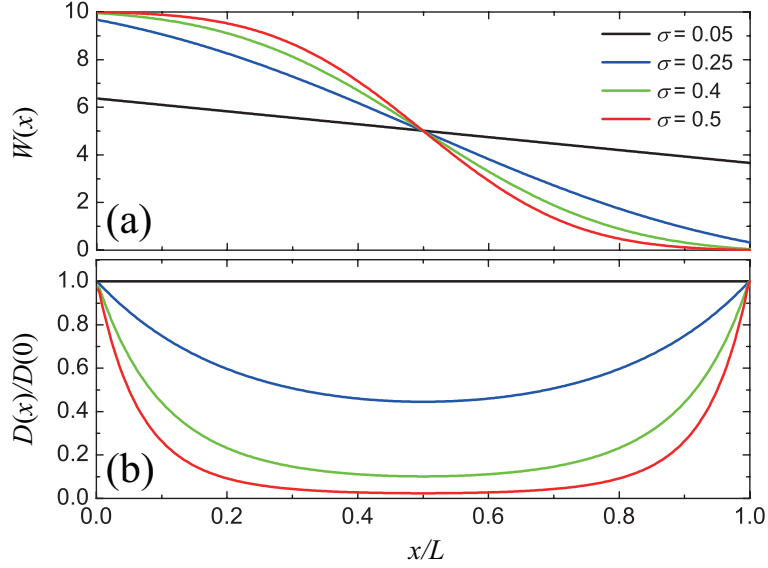


Figure 5: Energy density profiles are shown in (a) for 4 different $\sigma = 0.05, 0.25, 0.4$ and 0.5 , with the sample length fixed at $L = 400/k_0$; Local diffusion coefficients normalized by the diffusion constant on the incident surface of sample, which are obtained from the energy densities are shown in (b).

4 Conclusions

We have performed detailed investigations to show how the disorder influences the light transport properties in a quasi-1D random system. We calculated the disorder-modulated transport mean free path and found a scaling relation with the disorder strength parameter σ . With this relation the transport properties of light are considered, and we found that when the sample length is fixed, the disorder modulation enables the system to cover all the transport regimes. We also discussed the influence of the disorder modulation on the diffusion coefficient

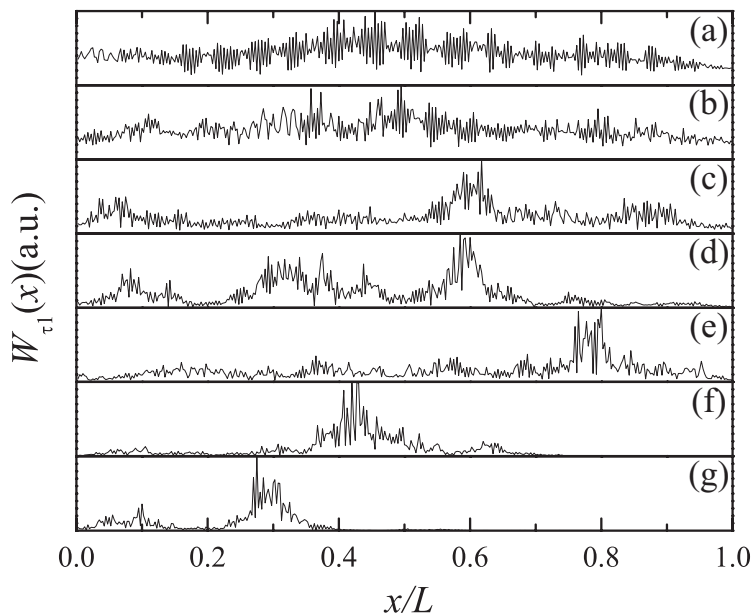


Figure 6: Normalized energy density profiles $W_{\tau_1}(x)$ of the eigenchannel with the maximal eigenvalue τ_1 for $\sigma^2 = 0.01, 0.025, 0.05, 0.1, 0.15, 0.2, 0.25$ (from top to bottom).

for samples with finite sizes, and confirmed that the diffusion is influenced by the strong inhomogeneous interference, especially in the localized regime.

This work is supported by the National Natural Science Foundation of China under Grant No. 11374063, and 973 Program(No. 2013CAB01505).

References

- [1] P. W. Anderson. Absence of diffusion in certain random lattices. *Phys. Rev.*, 109:1492–1505, Mar 1958.
- [2] Meint P. Van Albada and Ad Lagendijk. Observation of weak localization of light in a random medium. *Phys. Rev. Lett.*, 55:2692–2695, Dec 1985.
- [3] Pierre-Etienne Wolf and Georg Maret. Weak localization and coherent backscattering of photons in disordered media. *Phys. Rev. Lett.*, 55:2696–2699, Dec 1985.
- [4] Martin Störzer, Peter Gross, Christof M. Aegerter, and Georg Maret. Observation of the critical regime near anderson localization of light. *Phys. Rev. Lett.*, 96:063904, Feb 2006.

- [5] E. Abrahams, P. W. Anderson, D. C. Licciardello, and T. V. Ramakrishnan. Scaling theory of localization: Absence of quantum diffusion in two dimensions. *Phys. Rev. Lett.*, 42:673–676, Mar 1979.
- [6] Juliette Billy, Vincent Josse, Zhanchun Zuo, Alain Bernard, Ben Hambrecht, Pierre Lugan, David Clement, Laurent Sanchez-Palencia, Philippe Bouyer, and Alain Aspect. Direct observation of anderson localization of matter waves in a controlled disorder. *Nature*, 453(7197):891–894, June 2008.
- [7] Giacomo Roati, Chiara D’Errico, Leonardo Fallani, Marco Fattori, Chiara Fort, Matteo Zaccanti, Giovanni Modugno, Michele Modugno, and Massimo Inguscio. Anderson localization of a non-interacting bose-einstein condensate. *Nature*, 453(7197):895–898, June 2008.
- [8] F. Jendrzejewski, A. Bernard, K. Muller, P. Cheinet, V. Josse, M. Piraud, L. Pezze, L. Sanchez-Palencia, A. Aspect, and P. Bouyer. Three-dimensional localization of ultracold atoms in an optical disordered potential. *Nat Phys*, 8(5):398–403, May 2012.
- [9] Hefei Hu, A. Strybulevych, J. H. Page, S. E. Skipetrov, and B. A. van Tiggelen. Localization of ultrasound in a three-dimensional elastic network. *Nat Phys*, 4(12):945–948, December 2008.
- [10] Diederik S. Wiersma, Paolo Bartolini, Ad Lagendijk, and Roberto Righini. Localization of light in a disordered medium. *Nature*, 390(6661):671–673, December 1997.
- [11] A. A. Chabanov, M. Stoytchev, and A. Z. Genack. Statistical signatures of photon localization. *Nature*, 404(6780):850–853, April 2000.
- [12] K. Yu. Bliokh, Yu. P. Bliokh, V. Freilikher, A. Z. Genack, B. Hu, and P. Sebah. Localized modes in open one-dimensional dissipative random systems. *Phys. Rev. Lett.*, 97:243904, Dec 2006.
- [13] Tal Schwartz, Guy Bartal, Shmuel Fishman, and Mordechai Segev. Transport and anderson localization in disordered two-dimensional photonic lattices. *Nature*, 446(7131):52–55, March 2007.
- [14] Costanza Toninelli, Evangellos Vekris, Geoffrey A. Ozin, Sajeev John, and Diederik S. Wiersma. Exceptional reduction of the diffusion constant in partially disordered photonic crystals. *Phys. Rev. Lett.*, 101:123901, Sep 2008.
- [15] PA Mello, P Pereyra, and N Kumar. Macroscopic approach to multichannel disordered conductors. *Ann. Phys.*, 181(2):290–317, 1988.

- [16] B. A. van Tiggelen, A. Lagendijk, and D. S. Wiersma. Reflection and transmission of waves near the localization threshold. *Phys. Rev. Lett.*, 84:4333–4336, May 2000.
- [17] Chu-Shun Tian, Sai-Kit Cheung, and Zhao-Qing Zhang. Local diffusion theory for localized waves in open media. *Phys. Rev. Lett.*, 105:263905, Dec 2010.
- [18] Daniel S. Fisher and Patrick A. Lee. Relation between conductivity and transmission matrix. *Phys. Rev. B*, 23:6851–6854, Jun 1981.
- [19] A. MacKinnon. The calculation of transport properties and density of states of disordered solids. *Z. Phys. B*, 59(4):385–390, 1985.
- [20] Harold U. Baranger, David P. DiVincenzo, Rodolfo A. Jalabert, and A. Douglas Stone. Classical and quantum ballistic-transport anomalies in microjunctions. *Phys. Rev. B*, 44:10637–10675, Nov 1991.
- [21] Eric Akkermans and Gilles Montambaux. *Mesoscopic Physics of Electrons and Photons*. Cambridge University Press, 2007. Cambridge Books Online.
- [22] Richard Berkovits and Shechao Feng. Correlations in coherent multiple scattering. *Physics Reports*, 238(3):135–172, March 1994.
- [23] Pier A. Mello and A. Douglas Stone. Maximum-entropy model for quantum-mechanical interference effects in metallic conductors. *Phys. Rev. B*, 44(8):3559–3576, August 1991.
- [24] Alexander D. Mirlin. Statistics of energy levels and eigenfunctions in disordered systems. *Physics Reports*, 326(5?6):259–382, March 2000.
- [25] Ben Payne, Alexey Yamilov, and Sergey E. Skipetrov. Anderson localization as position-dependent diffusion in disordered waveguides. *Phys. Rev. B*, 82(2):024205–, July 2010.